Journal of Bioscience and Bioengineering
VOL. 129 No. 6, 756–764, 2020

ELSEVIER

www.elsevier.com/locate/jbiosc

Chondrogenic differentiation of mesenchymal stem/stromal cells on 3D porous poly (ε-caprolactone) scaffolds: Effects of material alkaline treatment and chondroitin sulfate supplementation

Carla Sofia Moura,[1,2] João Carlos Silva,[2,3] Sofia Faria,[4] Paulo Rui Fernandes,[4] Cláudia Lobato da Silva,[2] Joaquim Manuel Sampaio Cabral,[2] Robert Linhardt,[3] Paulo Jorge Bártolo,[5] and Frederico Castelo Ferreira[2,*]

CDRSP, Centre for Rapid and Sustainable Product Development, Polytechnic Institute of Leiria, Rua de Portugal-Zona Industrial, Marinha Grande, Portugal,[1] Department of Bioengineering and iBB-Institute for Bioengineering and Biosciences, Instituto Superior Técnico, Universidade de Lisboa, Lisbon, Portugal,[2] Department of Chemistry and Chemical Biology, Biological Sciences and Chemical and Biological Engineering, Center for Biotechnology and Interdisciplinary Studies, Rensselaer Polytechnic Institute, Troy, NY, USA,[3] Institute of Mechanical Engineering (IDMEC), Instituto Superior Técnico, University of Lisbon, Lisboa, Portugal,[4] and Manchester Biomanufacturing Centre, School of Mechanical and Aerospace and Civil Engineering, Manchester Institute of Biotechnology, University of Manchester, Manchester, United Kingdom[5]

Received 12 September 2019; accepted 21 January 2020
Available online 25 February 2020

Cartilage defects resultant from trauma or degenerative diseases (e.g., osteoarthritis) can potentially be repaired using tissue engineering (TE) strategies combining progenitor cells, biomaterial scaffolds and bio-physical/chemical cues. This work examines promoting chondrogenic differentiation of human bone marrow mesenchymal stem/stromal cells (BM-MSCs) by combining the effects of modified poly (ε-caprolactone) (PCL) scaffolds hydrophilicity and chondroitin sulfate (CS) supplementation in a hypoxic 5% oxygen atmosphere. 3D-extruded PCL scaffolds, characterized by μCT, featured a 21 mm^{-1} surface area to volume ratio, 390 μm pore size and approximately 100% pore interconnectivity. Scaffold immersion in sodium hydroxide solutions for different periods of time had major effects in scaffold surface morphology, wettability and mechanical properties, but without improvements on cell adhesion. *In-situ* chondrogenic differentiation of BM-MSC seeded in 3D-extruded PCL scaffolds resulted in higher cell populations and ECM deposition along all scaffold structure, when chondrogenesis was preceded by an expansion phase. Additionally, CS supplementation during BM-MSC expansion was crucial to enhance aggrecan gene expression, known as a hallmark of chondrogenesis. Overall, this study presents an approach to tailor the wettability and mechanical properties of PCL scaffolds and supports the use of CS-supplementation as a biochemical cue in integrated TE strategies for cartilage regeneration.

[**Key words:** Articular cartilage tissue engineering; Bone marrow mesenchymal stem/stromal cells; Chondroitin sulfate; Fused deposition modeling; Hypoxia; Poly (ε-caprolactone) scaffolds]

Articular cartilage is a unique connective tissue with a pivotal role in physiological mobility by providing a low friction surface for the mechanical load transmission between joints (1). Despite its complex structure, articular cartilage is mainly composed of chondrocytes encapsulated in a dense matrix of collagen and proteoglycans. Cartilage lacks vascularization and neural connections, which, upon injury after physical trauma or as result of degenerative diseases such as osteoarthritis (OA), limits its self-healing capacity through endogenous mechanisms (1,2). OA is the most prevalent joint disease associated with pain and disability, affecting more than 25% of the adult population (3). Additionally, current treatments, including microfracture, mosaicplasty or autologous chondrocyte implantation, often result in the formation of mechanically inferior fibrocartilage tissue instead of native-like hyaline cartilage and have been associated with limitations such as pain, donor site morbidity and inflammation (2,4). Tissue engineering (TE) approaches, combining progenitor cells, 3D biomaterial scaffolds and biochemical/physical factors, may constitute an effective alternative to address the unsolved issue of cartilage regeneration. TE strategies, following a better mimicking of the native microenvironment, are expected to achieve the development of functional articular cartilage with proper biochemical, structural and mechanical properties (5).

Mesenchymal stem/stromal cells (MSC) consist in an attractive alternative cell source to articular chondrocytes for cartilage TE strategies, as they are highly available, can be easily expanded, and, upon the application of relevant external stimuli, are capable to differentiate into cartilage (6). These cells also present specific features favoring a regenerative microenvironment, such as their low immunogenicity, and their trophic and immunomodulatory activity (7). MSC have been isolated from a wide variety of tissues such as bone marrow, adipose tissue, muscle, periosteum, umbilical cord matrix, intrapatellar fat pad and synovial membrane (8–11). In cartilage TE, bone marrow (BM)- and synovium-derived MSC have been described as the sources with the highest chondrogenic ability (8,12).

* Corresponding author. Tel.: +351 21 8419598; fax: +351 21 8419062.
E-mail address: frederico.ferreira@ist.utl.pt (F.C. Ferreira).

1389-1723/$ – see front matter
https://doi.org/10.1016/j.jbiosc.2020.01.004

Both natural and synthetic scaffolds have been widely studied for cartilage regeneration purposes (13). Natural scaffold materials are highly biocompatible, biodegradable and have multiple adhesion sites for cells. However, their uncontrolled degradation kinetics and poor mechanical properties represent important limitations for cartilage TE applications. In contrast, synthetic scaffolds can be manufactured with highly predictive properties (13,14). Control over TE scaffold properties has been clearly enhanced by the emergence of additive manufacturing (AM) techniques. AM techniques, such as melt extrusion/fused deposition modeling (FDM), offer a rapid and controlled method for producing tailor-made scaffolds with the desired shape, size and architecture to fit perfectly into a patient's defect site (14,15). In 3D extrusion/FDM, used for TE scaffold fabrication since 2000, thin thermoplastic filaments or granules of material are melted by heating and guided by a robotic device with computer-controlled motion, to generate a 3D construct (15).

Poly (ε-caprolactone) (PCL) is a synthetic thermoplastic, biodegradable and biocompatible material, which is approved by the FDA for several medical applications. PCL is an easy to process and chemically versatile linear aliphatic polyester with high thermal and structural stability (16–18). These properties combined with the fact that its degradation products can be harmlessly metabolized through the tricarboxylic acid cycle, has made PCL a suitable material for scaffold manufacturing in cartilage TE (17,18). However, the hydrophobic nature of PCL material can impair cellular attachment and compromise the success of the TE strategy (19). Several approaches have been examined to address this issue by increasing the hydrophilicity of PCL, including plasma and chemical treatments, blends with hydrophilic materials and incorporation of naturally derived extracellular matrix (ECM) molecules (19–26).

Aggrecan, a relatively large proteoglycan with many glycosaminoglycan (GAG) chains, consisting primarily of chondroitin sulfate (CS), represents the major proteoglycan component of cartilage ECM (27). In cartilage, constituent GAGs such as CS and hyaluronic acid (HA) play a crucial structural role as they are involved in protein–protein and cell–protein interactions within the ECM (27,28). Therefore, GAGs are important as molecular co-receptors in several biological processes such as cell adhesion, migration, proliferation, signaling and differentiation (28,29). Additionally, due to its high negative charge, CS plays an important role in cartilage swelling, enhancing the tissue ability to sustain mechanical loads (30). As result of these properties, CS has been studied as a biomimetic scaffold material for cartilage regeneration (25,26,31,32). In addition, CS has been also tested as a culture medium component to improve the biological function of chondrocytes (33).

In the present study, we produced 3D porous PCL scaffolds with high interconnectivities and used a very simple and inexpensive method, alkaline hydrolysis, to enhance scaffold hydrophilicity by increasing the hydrophilic terminal groups on the material surface. The effects of this treatment on scaffold structure, mechanical performance and wettability were evaluated. Finally, we investigated the effect of CS supplementation during the expansion phase on the chondrogenic differentiation of bone marrow mesenchymal stem/stromal cells (BM-MSCs) in alkaline-treated PCL scaffolds.

MATERIALS AND METHODS

Fabrication of PCL scaffolds PCL (MW 50000 Da, Capa, Perstorp, Caprolactone, UK) scaffolds were produced by 3D melt extrusion/FDM using the Bioextruder machine as described elsewhere (16,34). Briefly, 3D models with the desired size and properties were designed in CAD software (SolidWorks, Dassault Systèmes, Paris, France). A 0°–90° lay-down pattern was selected to obtain orthogonally aligned fibers and pores with a regular square geometry and pore size of 390 μm. The following extrusion process conditions were used: temperature of 80°C, slightly above PCL melting point, was employed to assure good interlayer adhesion; deposition velocity of 8 mm/s; rotation velocity of 22.5 rpm; slice thickness of 280 μm and a nozzle diameter of 300 μm, which corresponds to the diameter of the extruded fiber.

Micro-computed tomography analysis Morphological studies and internal microstructure images of the PCL scaffolds were obtained using a micro-computed tomography (μ-CT) equipment (SkyScan 1174v2, Bruker version 1.1, Bruker, Billerica, MA, USA) with the following acquisition parameters: image pixel size of 6.60 μm; source voltage of 50 kV; source current of 800 μA; exposure time of 2200 ms; rotation step of 0.7° (no filter). Image reconstruction was performed using NRecon Program Version 1.6.8.0 (Bruker). CTVox software (Bruker) was used to obtain a 3D realistic visualization of the scanned scaffold samples.

Alkaline treatment of PCL scaffolds PCL scaffolds were fully immersed in sodium hydroxide (NaOH, Sigma, St. Louis, MO, USA) 1 M aqueous solutions with exposure times of 1, 6 and 24 h. Pristine untreated scaffolds were used as control. After the exposure to NaOH solution, the scaffolds were rinsed at least three times with distilled water to ensure the finalization of the treatment.

Scanning electron microscopy NaOH-treated and pristine scaffolds were sputter-coated with a 45 nm gold/palladium layer (Quorum Technologies sputter coater, model E5100, Quorum Technologies, Lewes, UK) and imaged at 40× and 80× of magnification using a conventional Scanning electron microscopy (SEM) (model S2400, Hitachi, Tokyo, Japan) with an electron beam of 20 kV accelerating voltage.

Compressive mechanical testing PCL scaffolds (dimensions: 8.5 mm × 8.5 mm × 3 mm) were mechanically evaluated under compressive testing using an Instron machine (model 5544, Instron, Norwood, MA, USA) equipped with a 2 kN load cell and a 50 mm diameter cylindrical compression plate. An extension rate of 1 mm/min was used following the ASTM standards (35) using seven samples ($n = 7$) for each condition. Results obtained were analyzed using the Bluehill 3 software (Instron). The compressive modulus of elasticity was determined by calculating the slope of the initial linear region of the stress-strain curve.

Contact angle measurements Contact angle (CA) is defined by the intersection of the liquid-air interface and solid surface. CA value of 90° establish the boundary for classification of materials as hydrophobic or hydrophilic. Films were produced by dissolving PCL (10% wt) in chloroform (Merck, Darmstadt, Germany) and by promoting solvent evaporation overnight inside a chemical flow hood. PCL films/scaffolds were submitted to the different NaOH 1 M incubation periods, dried and maintained at room temperature until analysis. CA values were measured using a DSA25B goniometer (Krüss, Hamburg, Germany) by placing a drop of distilled water on the top of the film/scaffold and data was processed using the software Drop Shape Analysis 4 version 2.1 (Krüss). Measurements were performed in 5 different regions of each sample with duration of 20 s (films) or 30 s (scaffolds) to verify drop stability.

BM-MSC culture and seeding onto PCL scaffolds Human BM samples were obtained from three healthy male donors (ages ranging from 29 to 36 years) upon informed consent and BM-MSCs were isolated as previously described (9). BM-MSCs were thawed and cultured under standard expansion conditions in Dulbecco's modified Eagle's medium (DMEM, Gibco Thermo Fisher Scientific, Waltham, MA, USA) with 10% v/v MSC qualified fetal bovine serum (FBS, Hyclone GE Healthcare, Chicago, IL, USA) and 1% v/v antibiotic-antimycotic (anti-anti, Gibco) at 37°C/5% CO_2. Culture medium was fully renewed every 3 days and the cells were passaged when 80% confluence was reached. Before seeding, 24 h-NaOH treated-PCL scaffolds were sterilized by overnight UV exposure and ethanol 70% v/v washing. Afterwards, the scaffolds were rinsed three times with a phosphate buffered saline (PBS, Gibco) and 1% v/v anti-anti solution, placed in an ultra-low attachment 24-well plate (VWR, Monroeville, PA, USA) and incubated for 2 h with culture media. For cell seeding, a drop containing 8×10^4 BM-MSC (passage between 4 and 6) was placed on the top center of the scaffolds and incubated at 37°C/5% CO_2 for 1 h before addition of culture media. The scaffolds seeded with human BM-MSC were cultured in hypoxic conditions (37°C/5% CO_2/5% O_2) under 4 different protocols: I (expansion), DMEM with 10% v/v FBS and 1% v/v anti-anti for 28 days; II (chondrogenesis), StemPro chondrogenesis differentiation kit (Gibco) for 28 days; III (expansion/chondrogenesis), DMEM with 10% v/v FBS and 1% v/v anti-anti for 14 days, followed by 14-days culture with StemPro chondrogenesis differentiation kit; and IV (expansion with CS supplementation/chondrogenesis), DMEM with 10% v/v FBS supplemented with 1% w/v bovine cartilage chondroitin sulfate (CS, Sigma) and 1% v/v anti-anti for 14 days, followed by 14-days culture with StemPro chondrogenesis differentiation kit. Respective culture mediums were fully replaced every 3 days.

Cell proliferation assessment Cell adhesion and proliferation were monitored using the AlamarBlue assay (Thermo Fisher Scientific), following the manufacturer's guidelines. Briefly, scaffold samples were incubated with a 10% v/v AlamarBlue solution (prepared in culture media) during 2 h at 37°C/5% CO_2.

Afterwards, the solution fluorescence intensity was measured in a multiplate fluorometer (Infinite200 PRO, Tecan, Männedorf, Switzerland) with an excitation wavelength of 560 nm and emission wavelength of 590 nm. At least three scaffolds ($n = 3$) were considered for each experimental group and the fluorescence intensity for each scaffold sample was measured in triplicate. PCL scaffolds without cells were used as blank controls. Equivalent cell numbers were estimated using as calibration the correlation between measured fluorescence intensity values of AlamarBlue assay with counted cells (trypan blue exclusion method) cultured in standard tissue culture polystyrene 24-well plates (BD Falcon, Corning, NY, USA).

Alcian Blue staining Alcian Blue (Sigma) staining was used to identify sulfated GAGs (sGAGs). At the end of each protocol, the tissue constructs obtained were washed several times with PBS, fixed with 2% v/v paraformaldehyde (PFA, Sigma) for 20 min and incubated with a 1% v/v Alcian Blue solution (Sigma, prepared in 0.1 N HCl) for 1 h. Constructs were then rinsed twice with PBS, washed once with distilled water and imaged under a light microscope (Leica, DMI3000B, Leica, Wetzlar, Germany).

Collagen II immunofluorescence staining At the end of the experiment (day 28), the final tissue constructs obtained under the 4 different protocols were washed with PBS and fixed with 2% v/v PFA for 20 min. Afterwards, samples were washed three times (5 min each wash) with 1% bovine serum albumin (BSA, Sigma) v/v solution (in PBS) and blocked with 0.3% v/v Triton X-100, 1% v/v BSA, 10% v/v FBS solution (in PBS) for 45 min. The tissue constructs were then incubated with primary antibody for collagen II (1:200 v/v, mouse collagen II monoclonal antibody 6B3, Thermo Fisher Scientific) in 0.3% v/v Triton X-100, 1% v/v BSA, 10% v/v FBS solution (in PBS) for 3 h at room temperature. The samples were washed once with 1% v/v BSA (in PBS) and incubated with goat anti-mouse IgG secondary antibody AlexaFluor 546 (1:200 v/v, Thermo Fisher Scientific, in 1% v/v BSA solution) in the dark for 1 h at room temperature. Scaffolds were then washed twice with PBS, counterstained with 4,6-diamino-2-phenylindole (DAPI, Sigma–Aldrich, 1.5 μg/mL in PBS) solution for 5 min, washed with PBS, and imaged under confocal fluorescence microscopy (Zeiss LSM 710, Zeiss, Oberkochen, Germany).

Quantitative real-time PCR analysis Total RNA was isolated from the final tissue constructs using the RNeasy Mini Kit (Quiagen, Hilden, Germany) and cDNA was synthetized from up to 1 μg of RNA using the High-Capacity cDNA Reverse Transcription kit (Applied Biosystems, Foster City, CA, USA) following the manufacturers' guidelines. Quantitative real-time PCR analysis was performed using the Fast SYBR Green Master Mix (Applied BioSystems) according to manufacturer's recommendations. PCR reactions were run in triplicate, using the StepOne RT-PCR System (Applied BioSystems). Targets included the marker genes Collagen type I (*COL1A1*), Collagen type II (*COL2A1*), Aggrecan (*ACAN*), *SOX9* and Collagen type X (*COL10A1*). The target genes expressions were normalized against the housekeeping gene *GAPDH* of the same condition and fold differences in expression levels were calculated relatively to protocol I using the $2^{-\Delta\Delta CT}$ method. The primer sequences used in the analysis are specified in Table 1.

Statistical analysis Results are presented as mean ± standard deviation (SD). The statistical analysis was performed using the analytical features of GraphPad Prism 7 software (GraphPad Software, San Diego, CA, USA). Statistically significant differences between independent samples were assessed by one-way ANOVA followed by Tukey post-hoc test. Unless stated otherwise, three experimental replicates ($n = 3$) were performed and statistically different values were considered for p-value < 0.05 (* $p < 0.05$, ** $p < 0.01$ and *** $p < 0.001$).

TABLE 1. Primer sequences used for quantitative real time PCR analysis of chondrogenic marker genes.

Target gene	Primer	Sequence
Collagen I (*COL1A1*)	Fwd	TGACGAGACCAAGAACTG
	Rev	CCATCCAAACCACTGAAACC
Collagen II (*COL2A1*)	Fwd	GTGGAGCAGCAAGAGCAAGGA
	Rev	CTTGCCCCACTTACCAGTGTG
Aggrecan (*ACAN*)	Fwd	CACGCTACACCCTGGACTTG
	Rev	CCATCTCCTCAGCGAAGCAGT
SOX9	Fwd	TTCATGAAGATGACCGACGA
	Rev	CACACCATGAAGGCGTTCAT
Collagen X (*COL10A1*)	Fwd	CCAGGTCTGGATGGTCCTA
	Rev	GTCCTCCAACTCCAGGATCA
GAPDH	Fwd	GGTCACCAGGGCTGCTTTTA
	Rev	CCTGGAAGATGGTGATGGGA

RESULTS

Fabrication and characterization of 3D-extruded porous PCL scaffolds PCL scaffolds (Fig. 1A) produced by 3D extrusion/FDM presented a highly controlled architecture. The μ-CT analysis (Fig. 1B) allows to establish that the produced scaffolds have a reproducible microstructure comprised of sharp fibers with 300 μm diameter and pore size of 390 μm, defined by the orthogonal structure designed (0–90° between fibers in two consecutive layers). Scaffold porosity around 57%, surface area to volume ratio of approximately 21 mm^{-1} and pore interconnectivity nearly 100% were estimated (Fig. 1C).

Effects of alkaline treatment on PCL scaffold surface morphology, mechanical performance and material hydrophilicity SEM images in Fig. 2 show increasing levels of

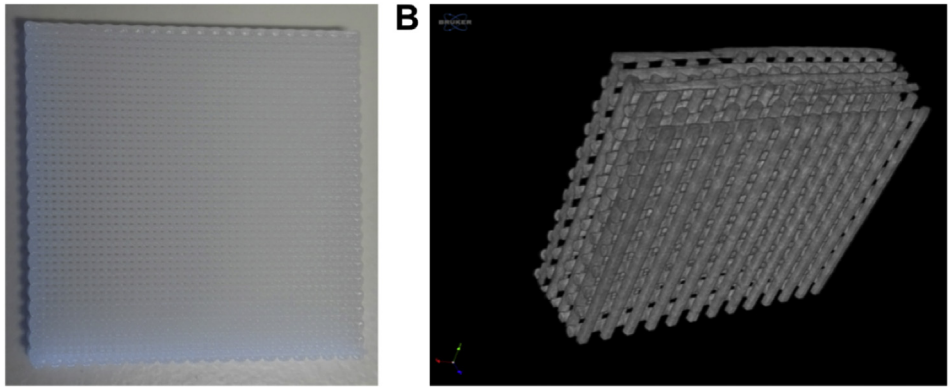

C

Scaffold estimated properties	
Porosity (%)	56.6
Surface area to volume ratio (mm^{-1})	21.2
Interconnectivity (%)	99.7

FIG. 1. PCL scaffolds fabricated by 3D extrusion. (A) Photograph of PCL scaffold. (B) 3D reconstructed image of a PCL scaffold upon μ-CT analysis. (C) Scaffold structural features estimated by μ-CT analysis.

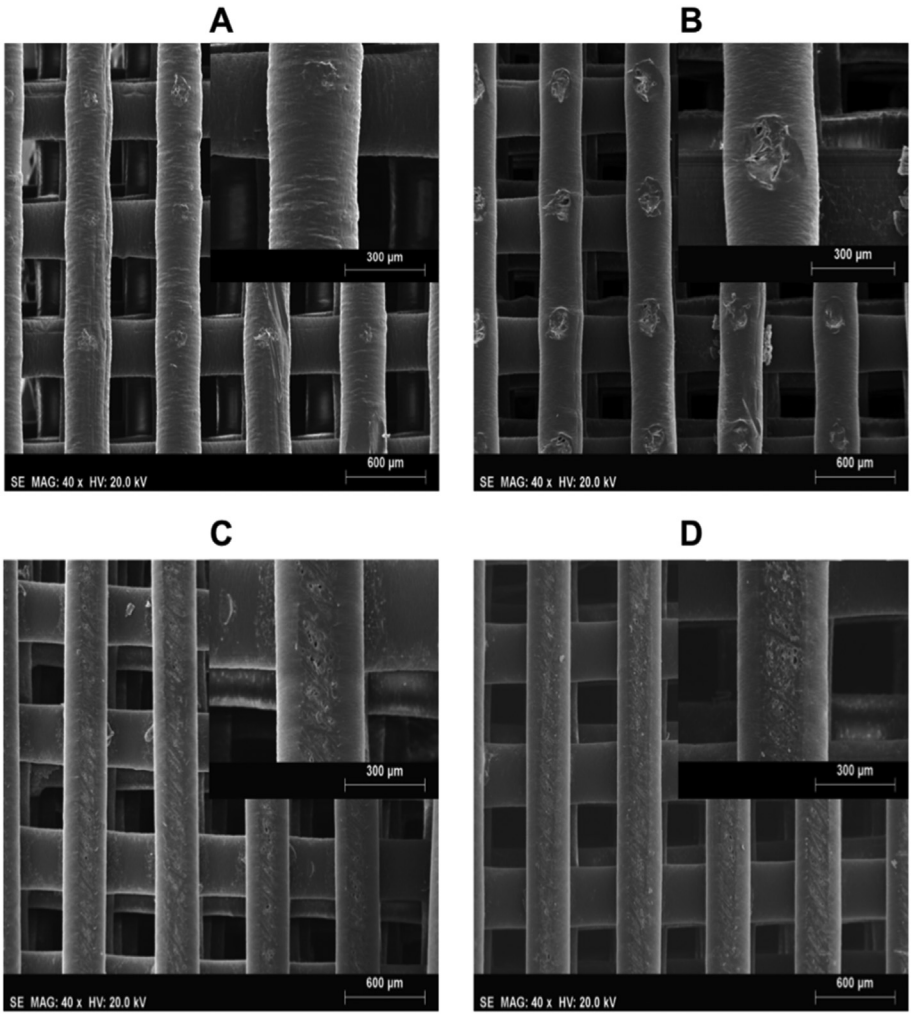

FIG. 2. SEM micrographic images of (A) untreated, (B) NaOH 1 M 1 h-, (C) NaOH 1 M 6 h- and (D) NaOH 1 M 24 h-treated-PCL scaffolds, including a wider observation and an amplified region (inside box, top right). Scale bars: 600 μm for the wider image and 300 μm for zoomed region image.

erosion of the PCL fibers surface with time of exposure to NaOH 1 M solution. However, the overall architecture of the alkaline treated-PCL scaffolds (Fig. 2B–D) was not considerably affected, remaining quite similar to the observed for the untreated sample (Fig. 2A). The stress-strain curves of PCL scaffolds submitted for different periods to NaOH 1 M solutions are quite different to the one obtained for the pristine scaffold (Fig. 3A), resulted in statistically different values of scaffolds compressive modulus (Fig. 3B). Accordingly, PCL scaffolds submitted to alkaline hydrolysis for 24 h presented a compressive modulus of 18.2 ± 0.84 MPa, nearly 40% lower than the value obtained for the pristine scaffolds (30.0 ± 1.45 MPa).

The contact angle (CA) between water and PCL material was estimated for the different alkaline treatment times in both film (Fig. 3C) and 3D-extruded scaffold configurations (Supplementary material Fig. S1). CA of PCL films surfaces submitted to alkaline hydrolysis were assessed, confirming an increase of material wettability with the time of exposure. CA ranging from hydrophobic values in untreated PCL films (CA = 100 ± 16° (t = 0 s) and CA = 107 ± 14° (t = 20 s)) and hydrophilic (CA = 30 ± 7° (t = 0 s) and CA = 29 ± 5° (t = 20 s)) after a 24 h-NaOH 1 M treatment were observed (Fig. 3C). Additionally, PCL scaffolds surface, initially hydrophobic (CA = 136 ± 22° (t = 0 s) and CA = 140 ± 16° (t = 30 s)), becomes hydrophilic after 24 h-NaOH 1 M treatment (CA = 47 ± 42° (t = 0 s) and 37 ± 28° (t = 30 s)) (Supplementary material Fig. S1). For exposure times longer than 24 h, the sessile water drop deposited in the scaffold surfaces, completely wetted the samples instantly. Interestingly, after 6 h of alkaline hydrolysis, 3D-extruded fibrous scaffold are still hydrophobic, but PCL films become already hydrophilic. The improvement in PCL scaffolds hydrophilicity after 24 h-NaOH treatment did not result in an increase in BM-MSC adhesion efficiency, with no meaningful differences between the number of equivalent cells adhering to NaOH-treated and pristine scaffolds (Fig. S2).

Effects of CS supplementation on BM-MSC proliferation and chondrogenic differentiation in PCL scaffolds Before the assessment of the effect of CS supplementation on BM-MSC proliferation and chondrogenic differentiation in 24 h NaOH 1 M-treated PCL scaffolds, an experimental assay was conducted to evaluate the impact of oxygen tension on BM-MSC proliferation in PCL scaffolds cultured under protocols II and III (Fig. S3). BM-MSC were seeded on pristine PCL scaffolds and cultured either under normoxic (21% O_2) or hypoxic (5% O_2) environment. Under culture protocol II, no major differences in equivalent cell numbers over time were observed between the tissue constructs obtained under different oxygen tensions. When considering a two-stage protocol (protocol III), hypoxia (5% O_2) conditions promoted considerably higher final equivalent cell numbers in PCL scaffolds than the ones obtained

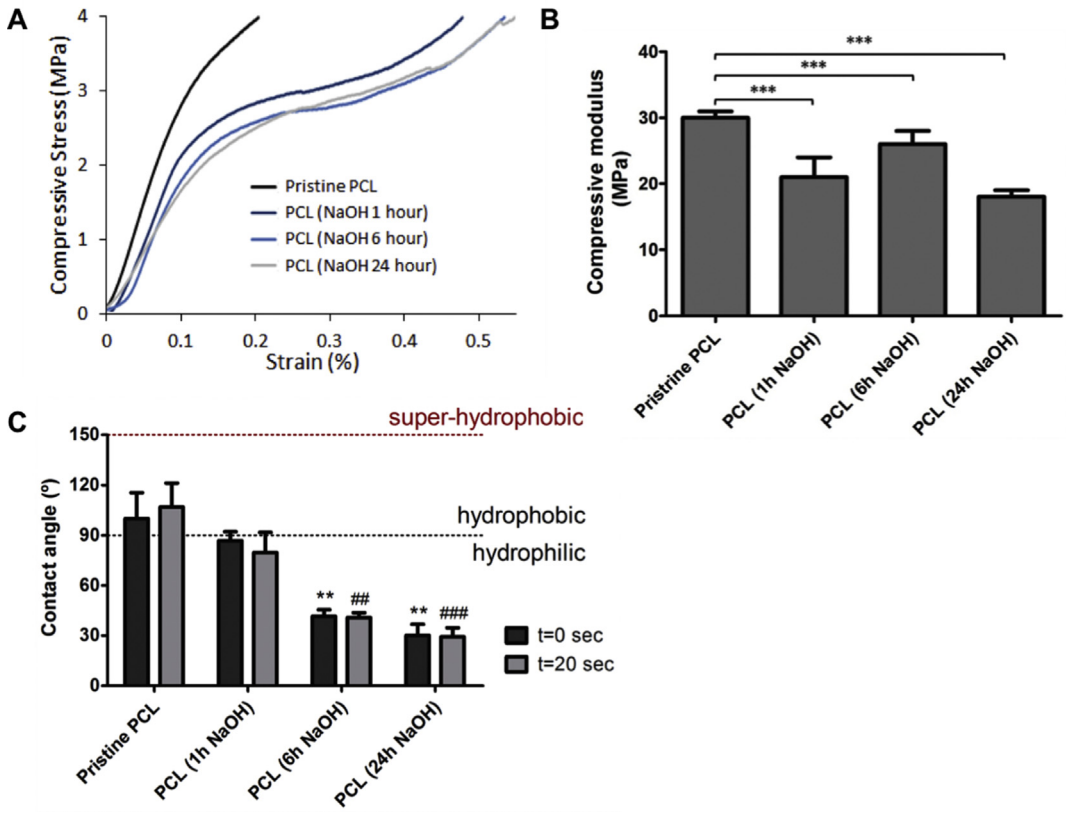

FIG. 3. Effect of alkaline hydrolysis time exposures on PCL scaffold mechanical properties and PCL material hydrophilicity. (A) Representative stress-strain curves of pristine and NaOH-treated PCL scaffolds. (B) Compressive modulus of pristine and NaOH-treated PCL scaffolds. Results are presented as mean ± standard deviation, from $n = 7$ independent measurements for each condition. Statistical significance was defined as $^{***}p < 0.001$, compared to pristine PCL. (C) Water contact angle (CA) values for pristine and NaOH 1 M-treated PCL films, measured at $t = 0$ s and $t = 20$ s. Results are shown as mean ± standard deviation of five measurements ($n = 5$) performed in different regions of the PCL films. Statistical significance was defined as $^{**}p < 0.01$ and $^{\#\#}p < 0.01$ or $^{\#\#\#}p < 0.001$, compared to control for $t = 0$ s and $t = 20$ s, respectively.

under normoxia (Fig. S3). Therefore, the effects of CS supplementation on BM-MSC proliferation and chondrogenesis were evaluated under a two-stage culture protocol under a hypoxic environment (5% O_2).

In the CS supplementation experimental assay, weekly equivalent cell numbers evolution over time is presented in Fig. 4. In addition, a curve representation of equivalent cell numbers over time and the weekly fold increase values (related to the first day of culture) are summarized in Fig. S4 and Table S1, respectively. When BM-MSC are cultured under protocol I for 28 days, equivalent cell numbers presented a fold increase of about 5.6 ± 0.22. The cell proliferation profile is quite similar for the first 14 days of expansion in protocols I and III, but for protocol III a slightly steeper decrease in equivalent cell numbers is observed on the 14 days of differentiation stage, reaching a final fold increase of 5.0 ± 0.69. When a single differentiation stage is used (protocol II), equivalent cell numbers start by increasing, then decrease slightly and finally stabilize until the end of the culture, corresponding to a final fold increase of 2.7 ± 0.24. Protocol IV used to assess the effect of CS addition in the expansion phase of the two-stage culture method, resulted in a final fold increase of 5.7 ± 0.47 in cell numbers, a value similar to the ones obtained under protocols I and III. Worth to notice, in protocol IV, despite an initial slower proliferation, equivalent cell numbers consistently increase over time; contrary to the other protocols studied where cell numbers oscillate over culture time (Figs. 4 and S4, Table S1).

The relative expressions of chondrogenic marker genes in the final tissue engineered constructs are presented in Fig. 5. The effect of chondrogenic medium use is stringent, with lower *COL1A1* expressions for any of the protocols using such medium, relatively to protocol I. *ACAN* expression was dramatically increased with the addition of CS (protocol IV) in comparison to any of the other protocols. *SOX9* expression appears to be favored by a two-stage

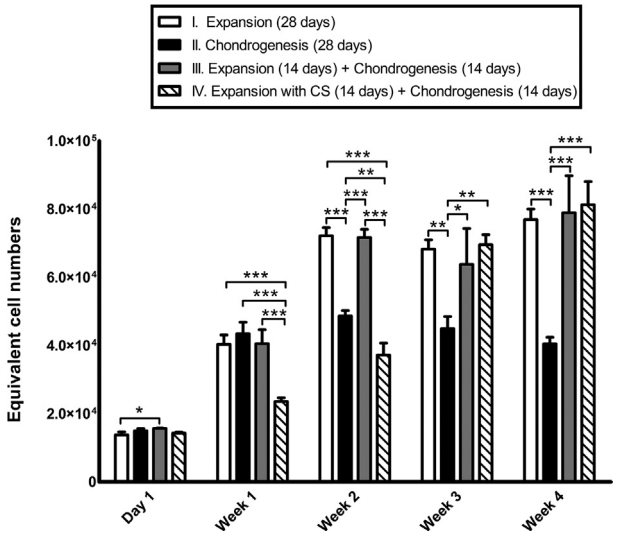

FIG. 4. BM-MSC proliferation on 24 h-NaOH 1 M treated-PCL scaffolds cultured under hypoxia (5% O_2 tension) for the four protocols studied. Results are represented as mean ± standard deviation ($n = 3$ independent experiments). Statistical significant differences in equivalent cell numbers between conditions within the same timepoint are defined as $^{*}p < 0.05$, $^{**}p < 0.01$ and $^{***}p < 0.001$.

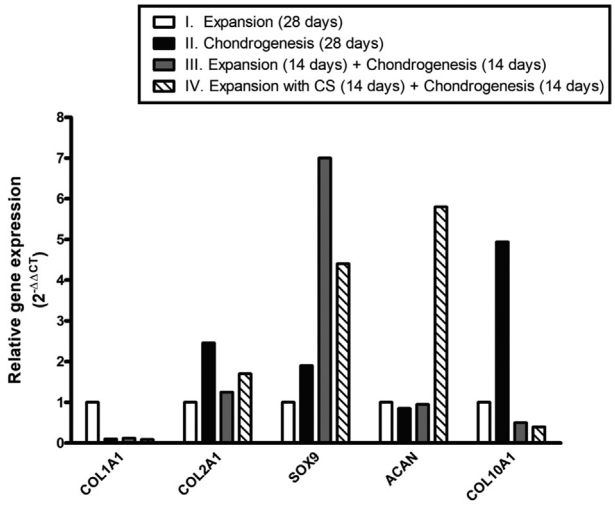

FIG. 5. Evaluation of BM-MSC chondrogenic differentiation on 24 h-NaOH 1 M treated-PCL scaffolds under the four protocols studied. Gene expression of *COL1A1*, *COL2A1*, *SOX9*, *ACAN* and *COL10A1* evaluated at the end of the four differentiation protocols (day 28) by quantitative real time PCR analysis. Gene expressions are normalized against the housekeeping gene *GAPDH* and presented as fold-change levels relative to protocol I.

protocol, as suggested by the higher expression observed in protocols III and IV. *COL2A1* expression levels were similar among protocols I and III, while slightly higher for protocol IV and highest in protocol II. A two-stage protocol appears to reduce hypertrophy, as suggested by the lower expressions of *COL10A1* hypertrophic marker observed in protocols III and IV, when compared to protocol II. Moreover, comparing *COL10A1* expression in protocols III and IV, it is suggested that CS supplementation might favor a less hypertrophic phenotype.

An additional experiment was performed to elucidate the effects of PCL scaffold alone on BM-MSC fate (Supplementary material Fig. S5). Chondrogenic markers expression was assessed by quantitative real-time PCR analysis, relatively to the initial cell population (BM-MSC prior to scaffold seeding – day 0), for cells obtained after three weeks culture on 24 h-NaOH 1 M treated PCL scaffolds using standard MSC expansion medium at 5% O_2 atmosphere. Results showed that the cells expanded on PCL scaffolds present a more chondrocyte-like genotype than the initial BM-MSC population, as suggested by the enhanced gene expressions, slightly for *COL2A1*, and considerably for *SOX9* and *ACAN*. Moreover, *COL1A1* expression in the obtained tissue constructs decreased slightly compared to the initial cell population.

Alcian Blue staining (Figs. 6A and S6) shows sGAG deposition at higher levels for protocols II, III and IV, in comparison to protocol I, in which a much less intensive staining was observed. However, samples generated under two-stage protocols III and IV, showed sGAG distribution throughout all scaffold structure, filling completely the scaffold pores, which was not verified for the samples obtained under protocol II. Additionally, as shown in Figs. 6B and S7, all sample groups stained positively for the presence of main articular cartilage protein collagen II.

DISCUSSION

The current study suggests a strategy to obtain cartilage-like tissue using 3D-extruded PCL scaffolds combined with BM-MSC, to provide insights for further design rapid prototyping approaches for cartilage regeneration tailored to patient defect specificities. The 3D-extruded PCL scaffolds architecture and fabrication methodology used were previously established and applied in bone TE (16,36). MSC osteogenesis is privileged by cell adhesion and stretching on hard material surfaces, while chondrogenesis usually proceeds through the formation of cell

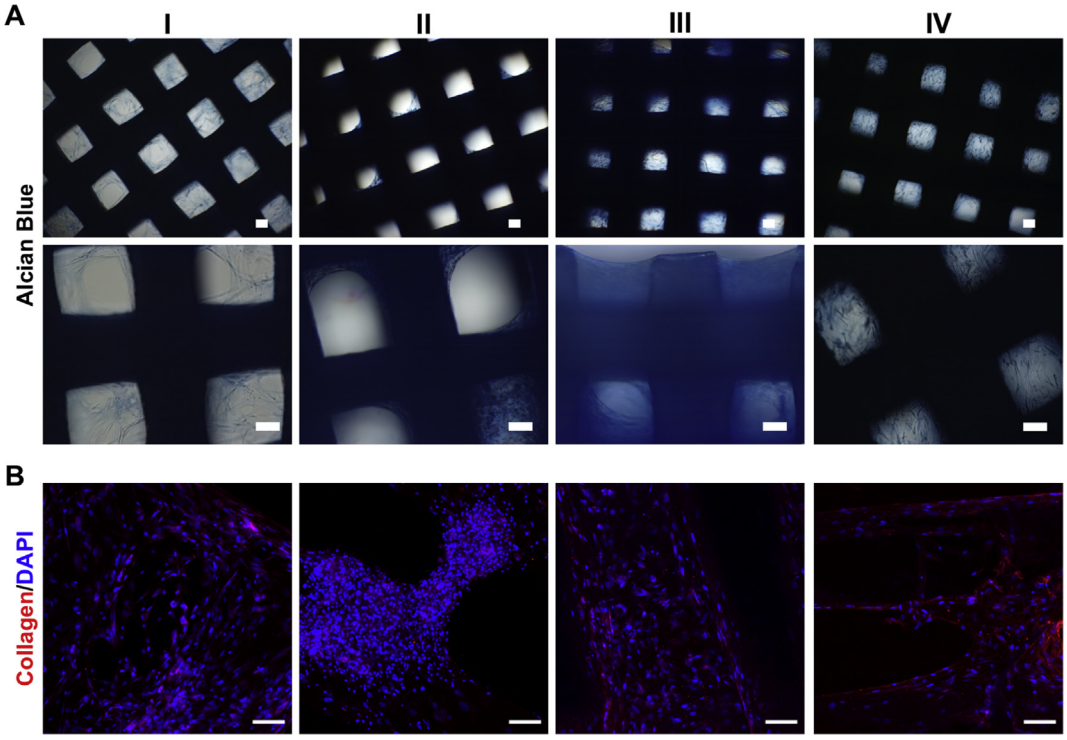

FIG. 6. Evaluation of typical cartilage ECM production after BM-MSC chondrogenic differentiation on 24 h- NaOH 1 M treated-PCL scaffolds under the four protocols studied (day 28). Representative images of Alcian Blue staining for sulfated GAGs at two different magnifications (A) and immunofluorescence analysis for type II collagen (B). Immunofluorescence samples were counterstained with DAPI. Scale bars: 100 μm.

aggregates. In the current study, we successfully established CS supplementation as an efficient strategy to obtain 3D-extruded PCL scaffolds with higher number of cells, while promoting *ACAN* expression and ECM deposition; and explored the use of a hydrolysis treatment as a valuable approach to increase PCL scaffold hydrophilicity, while decreasing its compressive modulus.

3D-extruded PCL scaffolds were fabricated with a larger pore size of 390 μm than in previous studies targeting osteogenesis (36). These dimensions were selected to allow not only metabolites, growth factors and cell migration along the whole scaffold, but also to accommodate GAG build up between the fibers. μ-CT reconstruction shows good consistency between real and theoretical values for scaffold structure and it was used to estimate relevant scaffold properties, usually postulated according to the fabrication parameters (16). An estimated scaffold porosity of nearly 57% is in agreement with previous works and was taken as an acceptable value, considering further material biodegradation and the structural integrity of the scaffold necessary to sustain mechanical and biological requirements (37). Surface area to volume ratio was estimated at a value about 21 mm^{-1}, providing a reasonable area for cell attachment, spreading and growth. A superior feature of this scaffold is its pore interconnectivity estimated at a value of 99.7%, an extremely high value compared with the ones obtained using conventional techniques (38). This remarkable property was privileged in the initial scaffold design to allow effective cell colonization throughout the entire scaffold surface and ECM deposition within the pores throughout the full 3D structure, and also to mitigate diffusion and nutrient supply limitations.

PCL was used for scaffold fabrication, since it is a relatively non-expensive FDA-approved material and its time frame for *in vivo* biodegradation has been shown appropriate to support cartilage regeneration (39). PCL scaffolds were submerged in NaOH 1 M solutions aiming at the hydrolysis of some of the PCL ester bonds into hydroxyl and carboxyl groups. Such approach had been previously carried out on PCL scaffolds aiming to improve cell adhesion through tuning surface hydrophilicity and roughness (22,40). Indeed, PCL surface hydrophilicity and roughness increased with longer contact time between PCL and alkaline solution, as indicated by the measured CA values, which is consistent with previous reports (22). However, contrary to the expected, increase on these features did not contribute to an improvement on cell adhesion efficiency. Still, the post-manufacturing alkaline scaffold treatment significantly increased hydrophilicity and decreased compressive modulus (Fig. 3B), which can be important on the broader context of a multilayer cartilage tissue construct. Interestingly, presenting carboxylic groups to MSC has been reported as a strategy to promote MSC chondrogenic differentiation (24,41,42). For example, Curran's work showed that carboxyl modified surfaces promoted collagen II expression by MSC, even when only basal medium was used (41).

The CA measured for the alkaline-treated porous PCL scaffolds presented high associated error bars, which can be explained by water droplet deformation by the fibers geometry. Still, the scaffolds are definitely hydrophilic after a 24 h-NaOH 1 M treatment. A bulk erosion has been described for PCL scaffolds (39). In this study, the alkaline attack to the PCL scaffolds seems to induce a pitting erosion after 1 h of treatment, with an extended fiber area affected for longer hydrolysis periods. As the scaffold becomes more hydrophilic, water transport and bulk erosion becomes facilitated. After 24 h-NaOH 1 M hydrolysis, scaffold's compressive modulus decreases from approximately 30 MPa18 MPa (about 40% of the initial value). However, the overall structure and architecture of the scaffold seems not to be affected. This is probably due to the semi-crystalline nature of PCL with slow degradation in well-organized and packed crystalline regions and faster hydrolysis of amorphous regions. Lam et al. (43) had reported decreases in compression modulus and yield stress to be accompanied by increases in crystallinity over several weeks of PCL alkaline hydrolysis. The decrease of scaffold stiffness resulted from the degradation of PCL ester bonds at a molecular level making the polymer chains shorter, but potentially also effects on the scaffold structure response to mechanic stimuli as eroded fibers changed format (43). Previous studies, using finite element analysis, described the relation between 3D-extruded PCL scaffolds structure and mechanical deformation (44). PCL scaffold compressive modulus, after 24 h-NaOH 1 M hydrolysis, is still remaining considerably higher than native hyaline cartilage modulus (0.53–1.82 MPa) (45). However, it is important to note that native hyaline cartilage is composed by three distinct layers (deep, middle and tangential zone), with its global mechanical properties depending on the interplay between the properties of each layer. The PCL scaffold herein studied aims to develop a bottom layer to mimic hyaline cartilage deep zone and provide appropriate structure and cellular organization at the osteochondral interface.

The use of MSC in cartilage regeneration settings addresses the limitations resulting from the monolayer culture instability and the low proliferative capacity of chondrocytes (5). Soluble signaling molecules included in the medium are usually the main driver to effectively direct MSC pathways towards specific linages (6). Currently, there are commercially available medium for MSC chondrogenic differentiation, ensuring quality control and reliability between batches, such as the StemPro A10071-01 used in this study. However, each lineage is favored not only by specific and complex networks of signaling molecules, but also by very different cell culture geometries. Cartilage and bone share the same osteochondro progenitors, and therefore, when promoting MSC differentiation usually there is a tight interplay between chondrogenesis and osteogenesis. *In vitro* MSC osteogenesis is favored by 2D monolayer cultures in hard surfaces where cells attach and spread, but MSC chondrogenesis requires cell condensation (46) and thus, it is better achieved in high density 3D cell aggregates or pellets. Such 3D cellular aggregates are usually obtained using the hanging drop technique or non-adherent micro-wells (6,47,48), which adds a cumbersome step on a potential TE product manufacturing line. Moreover, MSC proliferation in aggregates/pellets alone or encapsulated is extremely slow, requiring prior expansion of MSC to achieve clinically relevant numbers. 3D cell configurations lack the macrostructure to be implanted in cartilage defects and recent advances sought to address such question through direct 3D bioprinting of encapsulated cells in hydrogels (49) or MSC seeding in 3D polymeric scaffolds (50).

The use of 3D-extrusion/FDM is extremely appealing for cartilage TE approaches, because the scaffold can actually be designed to precisely fit the geometry of the chondral defect and guide tissue formation. Therefore, for almost two decades, the use of FDM scaffold approaches for cartilage regeneration has been suggested (20,51). Considering the extruded scaffolds structure, cells may tend to stretch on large hard fiber surfaces and commit to bone lineage, making extremely challenging to differentiate them towards cartilage on such PCL extruded scaffolds (52). To circumvent such limitation, different strategies have been followed: (i) differentiate MSC into chondrocytes using 3D pellet cultures before seeding on the scaffolds (53); (ii) integrate chondrocytes or MSC pellets in hydrogels, such as alginate (54,55) or thermosensitive PLGA–PEG–PLGA copolymer (56); (iii) coating the PCL fibers with GAGs (HA and CS) (25,26,57) or (iv) co-extrusion of PCL/hydroxyapatite (58). However, the bulk use of expensive biological materials increases costs, supply risks and quality control requirements.

Ideally, MSC should be directly seeded on the tailor-made scaffolds and after in-situ proliferation and chondrogenenic differentiation, implanted in the chondral defect site. For this strategy, it is essential to obtain, after the *in vitro* culture, a scaffold

populated with a relatively high number of cells committed with the chondrogenic lineage and able of cartilage-like ECM production. The scaffolds submitted to the two-stage differentiation protocol (III and IV) present almost twice the number of cells of the single-stage chondrogenesis (protocol II), matching the expansion control (protocol I), which indicates the first stage effectiveness on cell expansion.

COL1A1 and *SOX9* relative expressions suggest that the high proliferation in protocol III was not accompanied with commitment towards osteogenic lineage. However, the expressions on *COL2A1* and *ACAN*, at the level of the reference protocol I (using only expansion media) suggests that 14-days of culture in chondrogenic media (protocol III) were not enough to promote effective chondrogenesis. Moreover, the similar *ACAN* expression (late chondrogenic marker) on protocols I, II and III clearly point out the need to improve medium composition to induce a more mature differentiation state. The use of a single-differentiation stage (protocol II) resulted on a low number of cells and consequently, lower sGAG production restricted to the edges of the PCL scaffold fibres, as shown by Alcian Blue staining. Moreover, the selection of a two-stage protocol appears to be relevant to prevent final tissue hypertrophy. Such observations suggest the importance of using an initial expansion stage.

Quantitative real-time PCR analysis (relatively to the initial cell population – day 0) of BM-MSC expanded on 24 h-NaOH 1 M treated PCL scaffolds for three weeks in standard expansion medium at 5% O_2 was performed to assess the effect of scaffold material/structure on BM-MSC fate. The results indicate an increase, although modest, in *COL2A1* (early chondrogenic marker), more pronounced in *SOX9* and considerably higher in *ACAN* (late chondrogenic marker) expression levels, confirming that BM-MSC chondrogenesis is occurring at some extent, in spite of the absence of chondrogenic soluble factors. This observation is in line with the positive Alcian Blue staining, indicating sGAG deposition in constructs obtained with protocol I. In contrast, *COL1A1* expression only decreases slightly, which indicates that MSC differentiation is not effective or specific. As stated before, the carboxyl moiety can provide cues for MSC chondrogenesis (40,41) and hydrolysis of the PCL ester groups yield hydroxyl and carboxyl groups, which could be the underlying cue for this result. Moreover, considering this additional experimental results, the fold in chondrogenic marker gene expressions for the four protocols (estimated relatively to protocol I) should be interpreted as an incremental effect on chondrogenesis due to medium and supplementation (CS) effects and not the net gain in enhanced chondrogenic markers expression considering scaffold and medium synergies.

The two-stage protocols III and IV (with and without addition of CS in the expansion stage medium, respectively) reached similar final cell numbers. However, the culture paths to reach such outcome are very different, with slower growth over the first 14 culture days for protocol IV than protocol III, as probably CS directs MSC towards chondrogenic differentiation in an earlier moment of the culture. CS supplementation leads to a significant increase in chondrogenic marker *ACAN* expression, suggesting that this strategy represents an interesting balance between cell proliferation and differentiation on 3D-extruded PCL scaffolds.

In conclusion, the current study presents a strategy to promote BM-MSC proliferation, migration and chondrogenic differentiation in 3D-extruded PCL scaffolds. While the results of the present study require both *in vitro* and *in vivo* validation for application into clinical settings, they contribute to highlight the use of 3D extrusion/FDM scaffolds for MSC-based TE based strategies for cartilage regeneration. Such scaffolds can be precisely tailored to specific patients' defect site, while manufactured using PCL, a FDA affordable polymer, and avoiding the use of biological materials in bulk, which increase costs and burdens with certification and quality control. Additionally, the approach presented includes the use of a simple and inexpensive alkaline-treatment as a post-manufacturing technique to modify PCL scaffold properties and possibly provide additional cues for MSC chondrogenic differentiation. Finally, a two-stage protocol, including CS as a medium additive during the expansion phase, is suggested as an efficient method to obtain highly populated PCL constructs with cells able to produce cartilage-like ECM.

Supplementary data to this article can be found online at https://doi.org/10.1016/j.jbiosc.2020.01.004.

ACKNOWLEDGMENTS

This work was supported by FCT - Portuguese Foundation for Science and Technology through the projects UID/BIO/04565/2020, UID/Multi/04044/2019, UIDB/500022/2020, PTDC/BBB-BMC/5655/2014, and PRECISE – Accelerating progress toward the new era of precision medicine (PAC-PRECISE-LISBOA-01-0145-FEDER – 016394) and Stimuli2BioScaffold (FCT grant PTDC/EME-SIS/32554/2017). Funding received from Programa Operacional Regional de Lisboa 2020 (Project No. 007317), MIT Portugal Program and through project POCI-01-0145-FEDER-016800 is also acknowledged. Carla Sofia Moura and João Carlos Silva are also thankful to FCT for funding received through the scholarships SFRH/BD/73970/2010 and SFRH/BD/105771/2014, respectively.

References

1. **Ge, Z., Li, C., Heng, B. C., Cao, G., and Yang, Z.:** Functional biomaterials for cartilage regeneration, J. Biomed. Mater. Res. A, **100A**, 2526–2536 (2012).
2. **Madeira, C., Santhagunam, A., Salgueiro, J. B., and Cabral, J. M. S.:** Advanced cell therapies for articular cartilage regeneration, Trends Biotechnol., **33**, 35–42 (2015).
3. **Chen, D., Shen, J., Zhao, W., Wang, T., Han, L., Hamilton, J. L., and Im, H.-J.:** Osteoarthritis: toward a comprehensive understanding of pathological mechanism, Bone Res., **5**, 16044 (2017).
4. **Rai, V., Dilisio, M. F., Dietz, N. E., and Agrawal, D. K.:** Recent strategies in cartilage repair: a systematic review of the scaffold development and tissue engineering, J. Biomed. Mater. Res. A, **105**, 2343–2354 (2017).
5. **Vinatier, C., Mrugala, D., Jorgensen, C., Guicheux, J., and Noël, D.:** Cartilage engineering: a crucial combination of cells, biomaterials and biofactors, Trends Biotechnol., **27**, 307–314 (2009).
6. **Chamberlain, G., Fox, J., Ashton, B., and Middleton, J.:** Concise review: mesenchymal stem cells: their phenotype, differentiation capacity, immunological feature and potential for homing, Stem Cell, **25**, 2739–2749 (2007).
7. **Murphy, M. B., Moncivais, K., and Caplan, A. I.:** Mesenchymal stem cells: environmentally responsive therapeutics for regenerative medicine, Exp. Mol. Med., **45**, e54 (2013).
8. **Tan, A. R. and Hung, C. T.:** Concise review: mesenchymal stem cells for functional cartilage tissue engineering: taking cues from chondrocyte-based constructs, Stem Cells Transl. Med., **6**, 1295–1303 (2017).
9. **Dos Santos, F., Andrade, P. Z., Boura, J. S., Abecasis, M. M., da Silva, C. L., and Cabral, J. M. S.:** Ex vivo expansion of human mesenchymal stem cells: a more effective cell proliferation kinetics and metabolism under hypoxia, J. Cell. Physiol., **223**, 27–35 (2010).
10. **Soure, A. M., Fernandes-Platzgummer, A., Moreira, F., Lilaia, C., Liu, S.-H., Ku, P., Huang, Y.-F., Milligan, W., Cabral, J. M. S., and da Silva, C. L.:** Integrated culture platform based on a human platelet lysate supplement for the isolation and scalable manufacturing of umbilical cord matrix-derived mesenchymal stem/stromal cells, J. Tissue. Eng. Regen. Med., **11**, 1630–1640 (2016).
11. **Santhagunam, A., Dos Santos, F., Madeira, C., Salgueiro, J. B., and Cabral, J. M. S.:** Isolation and ex vivo expansion of synovial mesenchymal stromal cells for cartilage repair, Cytotherapy, **16**, 440–453 (2013).
12. **Sakaguchi, Y., Sekiya, I., Yagishita, K., and Muneta, T.:** Comparison of human stem cells derived from various mesenchymal tissues: superiority of synovium as a cell source, Arthritis Rheum., **52**, 2521–2529 (2005).
13. **Smith, B. D. and Grande, D. A.:** The current state of scaffolds for musculoskeletal regenerative applications, Nat. Rev. Rheumatol., **11**, 213–222 (2015).
14. **Melchels, F. P. W., Domingos, M. A. N., Klein, T. J., Malda, J., Bartolo, P. J., and Hutmacher, D. W.:** Additive manufacturing of tissues and organs, Prog. Polym. Sci., **37**, 1079–1104 (2012).
15. **Mota, C., Puppi, D., Chiellini, F., and Chiellini, E.:** Additive manufacturing techniques for the production of tissue engineering constructs, J. Tissue. Eng. Regen. Med., **9**, 174–190 (2015).

16. **Domingos, M., Chiellini, F., Gloria, A., Ambrosio, L., Bartolo, P. J., and Chiellini, E.:** Effect of process parameters on the morphological and mechanical properties of 3D Bioextruded poly (ε-caprolactone) scaffolds, Rapid Prototyp. J., **18**, 56–67 (2012).
17. **Kim, H. J., Lee, J. H., and Im, G.:** Chondrogenesis using mesenchymal stem cells and PCL scaffolds, J. Biomed. Mater. Res. A, **92**, 659–666 (2010).
18. **Woodward, S. C., Brewer, P. S., Moatamed, F., Schindler, A., and Pitt, C. G.:** The intracellular degradation of poly (ε-caprolactone), J. Biomed. Mater. Res. A, **19**, 437–444 (1985).
19. **Sousa, I., Mendes, A., Pereira, R. F., and Bartolo, P. J.:** Collagen surface modified poly (ε-caprolactone) scaffolds with improved hydrophilicity and cell adhesion properties, Mater. Lett., **134**, 263–267 (2014).
20. **Tiaw, K. S., Goh, S. W., Hong, M., Wang, Z., Lan, B., and Teoh, S. H.:** Laser surface modification of poly (ε-caprolactone) (PCL) membrane for tissue engineering applications, Biomaterials, **26**, 763–769 (2005).
21. **Martins, A., Pinho, E. D., Faria, S., Pashkuleva, I., Marques, A. P., Reis, R. L., and Neves, N. M.:** Surface modification of electrospun polycaprolactone nanofiber meshes by plasma treatment to enhance biological performance, Small, **5**, 1195–1206 (2009).
22. **Tsuji, H., Ishida, T., and Fukuda, N.:** Surface hydrophilicity and enzymatic hydrolyzability of biodegradable polyesters: effects of alkaline treatment, Polym. Int., **52**, 843–852 (2003).
23. **Neves, S. C., Teixeira, L. S. M., Moroni, L., Reis, R. L., van Blitterswijk, C. A., Alves, N. M., Karperien, M., and Mano, J. F.:** Chitosan/Poly (ε-caprolactone) (PCL) scaffolds for cartilage repair, Biomaterials, **32**, 1069–1079 (2011).
24. **Chen, M., Xu, L., Zhou, Y., Zhang, Y., Lang, M., Ye, Z., and Tan, W.-S.:** Poly (ε-caprolactone)-based substrates bearing pendant small chemical groups as a platform for systemic investigation of chondrogenesis, Cell Prolif., **49**, 512–522 (2016).
25. **Piai, J. F., Alves da Silva, M., Martins, A., Torres, A. B., Faria, S., Reis, R. L., Muniz, E. C., and Alves, N. M.:** Chondroitin sulfate immobilization at the surface of electrospun nanofiber meshes for cartilage tissue regeneration approaches, Appl. Surf. Sci., **403**, 112–125 (2017).
26. **Chang, K. Y., Hung, L. H., Chu, I. M., Ko, C. S., and Lee, Y. D.:** The application of type II collagen and chondroitin sulfate grafted PCL porous scaffold in cartilage tissue engineering, J. Biomed. Mater. Res. A, **92**, 712–723 (2010).
27. **Knudson, C. B. and Knudson, W.:** Cartilage proteoglycans, Semin. Cell Dev. Biol., **12**, 69–78 (2011).
28. **Raman, R., Sasisekharan, V., and Sasisekharan, R.:** Structural insights into biological roles of protein-glycosaminoglycan interactions, Chem. Biol., **12**, 267–277 (2005).
29. **Mathews, S., Mathew, S. A., Gupta, P. K., Bhonde, R., and Totey, S.:** Glycosaminoglycans enhance osteoblast differentiation of bone marrow derived human mesenchymal stem cells, J. Tissue Eng. Regen. Med., **8**, 143–152 (2014).
30. **Chahine, N. O., Chen, F. H., Hung, C. T., and Ateshian, G. A.:** Direct measurement of osmotic pressure of glycosaminoglycan solutions by membrane osmometry at room temperature, Biophys. J., **89**, 1543–1550 (2005).
31. **Varghese, S., Hwang, N. S., Canver, A. C., Theprungsirikul, P., Lin, D. W., and Elisseeff, J.:** Chondroitin sulfate based niches for chondrogenic differentiation of mesenchymal stem cells, Matrix Biol., **27**, 12–21 (2008).
32. **Chang, C. H., Liu, H. C., Lin, C. C., Chou, C. H., and Lin, F. H.:** Gelatin-chondroitin-hyaluronan tri-copolymer scaffold for cartilage tissue engineering, Biomaterials, **24**, 4853–4858 (2003).
33. **Stellavato, A., Tirino, V., de Novellis, F., Vecchia, A. D., Cinquegrani, F., De Rosa, M., Papaccio, G., and Schiraldi, C.:** Biotechnological chondroitin a novel glycosaminoglycan with remarkable biological function on human primary chondrocytes, J. Cell. Biochem., **117**, 2158–2169 (2016).
34. **Silva, J. C., Moura, C. S., Borrecho, G., Alves de Matos, A. P., da Silva, C. L., Cabral, J. M. S., Bártolo, P. J., Linhardt, R. J., and Ferreira, F. C.:** Extruded bioreactor perfusion culture supports the chondrogenic differentiation of human mesenchymal stem/stromal cells in 3D porous poly(ε-caprolactone) scaffolds, Biotechnol. J., **15**, 1900078 (2020).
35. **ASTM International:** Standard test method for compressive properties of rigid plastics, ASTM D695–02a. ASTM International, West Conshohocken, PA (2002).
36. **Patrício, T., Domingos, M., Gloria, A., D'Amora, U., Coelho, J. F., and Bartolo, P. J.:** Fabrication and characterisation of PCL and PCL/PLA scaffolds for tissue engineering, Rapid Prototyp. J., **20**, 145–156 (2014).
37. **Malda, J., Woodfield, T. B. F., van der Vloodt, F., Wilson, C., Martens, D. E., Tramper, J., van Blitterswijk, C. A., and Riesle, J.:** The effect of PEGT/PBT scaffold architecture on the composition of tissue engineered cartilage, Biomaterials, **26**, 63–72 (2005).
38. **Peltola, S. M., Melchels, F. P., Grijpma, D. W., and Kellomäki, M.:** A review of rapid prototyping techniques for tissue engineering purposes, Ann. Med., **40**, 268–280 (2008).
39. **Woodruff, M. A. and Hutmacher, D. W.:** The return of a forgotten polymer-Polycaprolactone in the 21st century, Prog. Polym. Sci., **35**, 1217–1256 (2010).
40. **Moutos, F. T., Glass, K. A., Compton, S. A., Ross, A. K., Gersbach, C. A., Guilak, F., and Estes, B. T.:** Anatomically shaped tissue-engineered cartilage with tunable and inducible anticytokine delivery for biological joint resurfacing, Proc. Natl. Acad. Sci., **113**, 4513–4522 (2016).
41. **Curran, J. M., Chen, R., and Hunt, J. A.:** The guidance of human mesenchymal stem cell differentiation in vitro by controlled modifications to the cell substrate, Biomaterials, **27**, 4783–4793 (2006).
42. **Benoit, D. S. W., Schwartz, M. P., Durney, A. R., and Anseth, A. R.:** Small functional groups for controlled differentiation of hydrogel-encapsulated human mesenchymal stem cells, Nat. Mater., **7**, 816–823 (2008).
43. **Lam, C. X. L., Savalani, M. M., Teoh, S. H., and Hutmacher, D. W.:** Dynamics of in vitro polymer degradation of polycaprolactone-based scaffolds: accelerated versus simulated physiological conditions, Biomed. Mater., **3**, 34108 (2008).
44. **Ribeiro, J. F. M., Oliveira, S. M., Alves, J. L., Pedro, A. J., Reis, R. L., Fernandes, E. M., and Mano, J. F.:** Structural monitoring and modeling of the mechanical deformation of three-dimensional printed poly (ε-caprolactone) scaffolds, Biofabrication, **9**, 25015 (2017).
45. **Bhosale, A. M. and Richardson, J. B.:** Articular cartilage: structure, injuries and review of management, Br. Med. Bull., **87**, 77–95 (2008).
46. **Kim, I. G., Ko, J., Lee, H. R., Do, S. H., and Park, K.:** Mesenchymal cells condensation-inducible mesh scaffolds for cartilage tissue engineering, Biomaterials, **85**, 18–29 (2016).
47. **Li, W. J., Tuli, R., Okafor, C., Derfoul, A., Danielson, K. G., Hall, D. J., and Tuan, R. S.:** A three-dimensional nanofibrous scaffold for cartilage tissue engineering using human mesenchymal stem cells, Biomaterials, **26**, 599–609 (2005).
48. **Martinez, I., Elvenes, J., Olsen, R., Bertheussen, K., and Johansen, O.:** Redifferentiation of in vitro expanded adult articular chondrocytes by combining the hanging-drop cultivation method with hypoxic environment, Cell Transplant., **17**, 987–996 (2008).
49. **Cui, X., Breitenkamp, K., Finn, M. G., Lotz, M., and D'Lima, D. D.:** Direct human cartilage repair using three-dimensional bioprinting Technology, Tissue Eng. Part A, **18**, 1304–1312 (2012).
50. **Seo, S. and Na, K.:** Mesenchymal StemCell-based tissue engineering for chondrogenesis, J. Biomed. Biotechnol., **2011**, 806891 (2011).
51. **Hutmacher, D. W., Schantz, T., Zein, I., Ng, K. W., Teoh, S. H., and Tan, K. C.:** Mechanical properties and cell cultural response of polycaprolactone scaffolds designed and fabricated via fused deposition modeling, J. Biomed. Mater. Res. A, **55**, 203–216 (2001).
52. **Shao, X., Goh, J. C. H., Hutmacher, D. W., Lee, E. H., and Zigang, G.:** Repair of large articular osteochondral defects using hybrid scaffolds and bone marrow-derived mesenchymal stem cells in a rabbit model, Tissue Eng., **12**, 1539–1551 (2006).
53. **Kock, L. M., Malda, J., Dhert, W. J., Ito, K., and Gawlitta, D.:** Flow-perfusion interferes with chondrogenic and hypertrophic matrix production by mesenchymal stem cells, J. Biomech., **47**, 2122–2129 (2014).
54. **Kundu, J., Shim, J. H., Jang, J., Kim, S. W., and Cho, D. W.:** An additive manufacturing-based PCL-alginate-chondrocyte bioprinted scaffold for cartilage tissue engineering, J. Tissue. Eng. Regen. Med., **9**, 1286–1297 (2015).
55. **Izadifar, Z., Chang, T., Kulyk, W., Chen, X., and Eames, B. F.:** Analyzing biological performance of 3D-printed, cell-impregnated hybrid constructs for cartilage tissue engineering, Tissue Eng. Part C Methods, **22**, 173–188 (2016).
56. **Wang, S.-J., Zhang, Z.-Z., Jiang, D., Qi, Y.-S., Wang, H.-J., Zhang, J.-Y., Ding, J.-X., and Yu, J.-K.:** Thermogel-coated poly(ε-caprolactone) composite scaffold for enhanced cartilage tissue engineering, Polymers, **8**, 200 (2016).
57. **Schagemann, J. C., Chung, H. W., Mrosek, E. H., Stone, J. J., Fitzsimmons, J. S., O'Driscoll, S. W., and Reinholz, G. G.:** Poly-caprolactone/gel hybrid scaffolds for cartilage tissue engineering, J. Biomed. Mater. Res. A, **93**, 454–463 (2010).
58. **Yao, Q., Wei, B., Liu, N., Li, C., Guo, Y., Shamie, A. N., Chen, J., Tang, C., Jin, C., Xu, Y., and other 3 authors:** Chondrogenic regeneration using bone marrow clots and a porous polycaprolactone-hydroxyapatite scaffold by three-dimensional printing, Tissue Eng. Part A, **21**, 1388–1397 (2015).